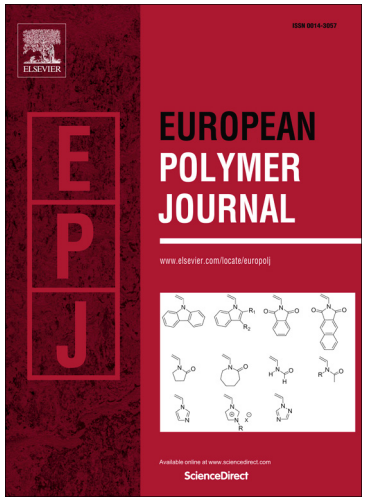

Functional PDMS enhanced strain at fracture and toughness of DGEBA epoxy resin

A. Romo-Uribe, K. Santiago-Santiago, A. Reyes-Mayer, M. Aguilar-Franco

PII: S0014-3057(16)31214-9
DOI: http://dx.doi.org/10.1016/j.eurpolymj.2017.01.041
Reference: EPJ 7711

To appear in: *European Polymer Journal*

Received Date: 2 October 2016
Revised Date: 20 January 2017
Accepted Date: 24 January 2017

Please cite this article as: Romo-Uribe, A., Santiago-Santiago, K., Reyes-Mayer, A., Aguilar-Franco, M., Functional PDMS enhanced strain at fracture and toughness of DGEBA epoxy resin, *European Polymer Journal* (2017), doi: http://dx.doi.org/10.1016/j.eurpolymj.2017.01.041

Submitted to *Eur Polym J* **EUROPOL_2016_1003R1** **Revised**

Functional PDMS enhanced strain at fracture and toughness of DGEBA epoxy resin

*A Romo-Uribe [1, †, *], K. Santiago-Santiago [2], A Reyes-Mayer [2] & M Aguilar-Franco [3]*

[1] Polymer Nanocomposites Laboratory, LNyC, Cuernavaca, Mor. 62230, MEXICO

[2] Universidad Tecnologica Emiliano Zapata del Estado de Morelos UTEZ, Av. Universidad Tecnologica No. 1, Col. Palo Escrito, Emiliano Zapata, Morelos, 62760, MEXICO

[3] Lab. Central de Microscopia, IFUNAM, Cd. Universitaria, Mexico DF 04510, MEXICO

[*] To whom all correspondence should be addressed. E-mail: aromouribe@gmail.com

[†] Now at R&D, Advanced Science & Technology Division, Johnson & Johnson Vision Care Inc., FL 32256, USA.

ABSTRACT

The thermo-mechanical properties of diglycidyl ether of bisphenol-A (DGEBA) epoxy / silyl-diglycidyl ether terminated polydimethyl siloxane (PDMS) composites have been investigated; PDMS concentration was increased up to 15 wt%. Differential scanning calorimetry (DSC) evidenced a phase separated microstructure as two glass transition temperatures, T_g, were detected: a high T_g at ca. 103°C corresponding to DGEBA phase, and a lower T_g at ca. 40°C. The lower T_g suggests interpenetration of PDMS into the DGEBA molecular network. SEM and AFM analyses confirmed the phase separated, droplet morphology, with well dispersed PDMS domains into the epoxy matrix. The PDMS droplets had diameters as small as 0.6 μm, and the droplet size increased up to ca. 1.8 μm at 15% PDMS content. Detailed EDS elemental mapping of the fractured composites evidenced siloxane residue in epoxy cavities suggesting incorporation of siloxane into the epoxy network, in agreement with DSC. Flexural testing showed a monotonic reduction of modulus (*E*) as PDMS content increased, as usually observed in rubber reinforced epoxy resins. However, strain at fracture and toughness increased twofold at about 10 wt% PDMS content. Water contact angle increased and then decreased as PDMS content increased, reaching maxima at ca. 10 wt% concentration. This behavior was apparently driven by surface roughness. The elastic mechanical modulus was found to scale with the droplet size of the rubbery phase.

Key words: epoxy, DGEBA, siloxane, microdomains, composites, mechanical properties

1. Introduction

Epoxy resins have found diverse applications in electronic, automotive and aerospace industries due to high chemical and corrosion resistance, good mechanical and thermal properties, outstanding adhesion to various substrates, low shrinkage upon cure, and good electrical insulating properties. [1] The addition of curing agents gives insoluble and intractable thermoset polymers which at the molecular scale consist of an interconnected molecular network. [2-5] However, epoxy resins are usually brittle and have low impact resistance, therefore efforts have been focused on toughness improvement by addition of elastomers. [6-9]

It has been shown that the rubber particle size in rubber-modified epoxy resins influences the toughness of the composite, significantly higher impact strength was found in the composite with 10-50 μm. [10, 11] Initially, the epoxy-rubber mixture has some degree of miscibility depending on their solubility parameters. However, as a molecular network forms during curing reaction, there is phase separation giving rise to epoxy-rich and rubber-rich phases. The control of phase separation and of rubber domains size, at a given concentration of rubber, determines ultimately the mechanical performance of the reinforced epoxy resin. [12-17] Rubber nanoparticles with pre-defined size (ca. 100 nm) recently reported can overcome the issue of phase separation and provided increase of toughness in epoxy resins [18]. However, the additional step of first synthesizing and characterizing the nanoparticles would be time consuming and not cost effective.

The search of epoxy formulations with resistance to high temperatures or moisture for long periods of time has led to the investigation of functional silanes, polysiloxanes, silsesquioxanes, and nanosilicas as possible reinforcers of epoxy resins. [19-29] For instance, it has been shown that poly(dimethylsiloxane) (PDMS) can be effective to improve the

thermomechanical properties and toughness of epoxy resins. [19, 27-29] Random siloxane copolymers have a low glass transition temperature (ca. -120°C), are hydrophobic, flexible, and thermally and oxidative stable. However, the solubility parameters of polysiloxanes can be quite different from epoxy giving rise to phase separation into large domains which do not increase fracture toughness. Hence, polysiloxanes with appropriate end groups which could promote compatibility with the epoxy phase have been investigated.

PDMS with compatible, functional end groups would reduce the rate of phase separation, incorporate to some extent into the crosslinked network, and therefore produce domains ca. 200 nm to 3 μm size, a size shown to be effective in enhancing fracture toughness [19, 28, 29], and reducing hardness [27].

The utilization of siloxanes with functional end groups has been the approach of this research program. The aim is to fine tune the thermal and mechanical properties of epoxy resins through the incorporation of tailored siloxanes in order to obtain tougher composites and nanocomposites for more demanding applications [27-29].

This research has led to the discovery that ether-terminated polydimethyl siloxane (PDMS-DGE) mixed with diglycidyl ether of bisphenol-A (DGEBA) and cured with 1,2-diaminocyclohexane (DCH) have given rise to either *composites* [27] or *nanocomposites* [28, 29] depending of the synthesis route. These syntheses routes are shown in scheme 1.

That is, it was shown that direct mixing of PDMS-DGE (and hydroxyl-terminated PDMS, denoted PDMS-co-DPS-OH) with DGEBA and cured with DCH was effective to produce *composites* with significantly reduced hardness. Furthermore, the curing kinetics was studied in detail by shear rheometry, and the results showed that both functional siloxanes (ether-terminated and hydroxyl-terminated) had an autocatalytic effect in the curing reaction which

significantly reduced the gel point time, relative to the neat epoxy. SEM showed that the final morphology of these composites, cured over a range of temperatures (90 to 140°C) consisted of well dispersed PDMS micro-droplets sized ca. 1-3 μm [27]. The final composites were optically opaque.

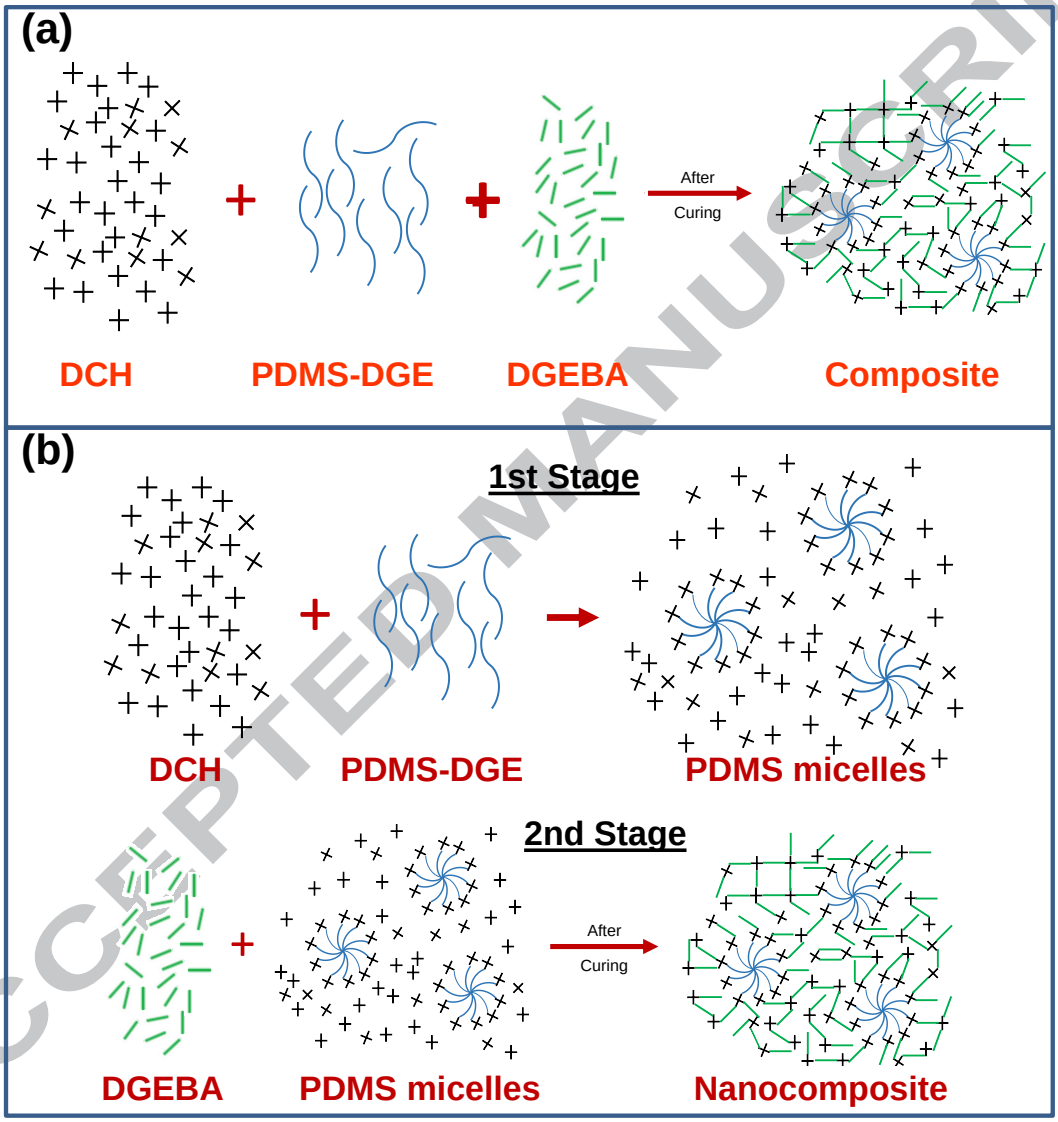

Scheme 1. Synthetic routes to obtain composites and nanocomposites using the same reactants, DGEBA epoxy, ether-terminated PDMS and curing agent DCH [27-29].

On the other hand, a facile method was developed in our lab to produce *nanocomposites* utilizing exactly the same reactants, PDMS-DGE, DGEBA and DCH [28, 29]. For this, PDMS-DGE was first pre-reacted with the hardener 1,2-diaminocyclohexane (DCH). During this pre-reaction stage the oxirane groups of PDMS were consumed, leaving only the amine groups of DCH available for further reaction. Then, the pre-reacted mixture was mixed with DGEBA and cured thus producing nanocomposites with strikingly enhanced flexural mechanical properties. Relative to the neat DGEBA, the nanocomposites exhibited a threefold increase in Young's modulus, the strain at fracture increased two-fold, and the toughness increased an order of magnitude, at only 5 wt% PDMS content. Transmission electron microscopy (TEM) showed that the final morphology of nanocomposites consisted of PDMS nano-domains with size averaging 200 nm [28, 29]. The final nanocomposites were optically transparent and hydrophobic.

This research now focuses on the influence of PDMS concentration on thermal and mechanical properties, and the correlation with the morphology of ether-terminated PDMS / DGEBA *composites*.

2. Experimental

2.1 Materials.

The epoxy resin was diglycidyl ether of bisphenol-A (DGEBA), with equivalent weight of epoxy group 170.2 g/eq, functionality of 2, molecular weight MW=340.41 g/mol, ρ=1.16 g/ml (25°C) and viscosity η=4000-6000 cP. 1,2-diaminocyclohexane (1,2-DCH) with 28.5 g/eq, functionality of 4, ρ=0.931 g/ml (25°C) and MW=114.19 g/mol was used as hardener. The liquid rubber was poly(dimethyl siloxane) diglycidyl ether terminated (PDMS-DGE) with 490 Eq./g, functionality of 2, MW~800 g/mol, ρ=0.99 g/ml (25°C) and η=15 cSt (25°C). The molecular

weight and viscosity values of the reactants are reported by the supplier, Sigma-Aldrich (St Louis MO, USA; sigma-aldrich.com). The reactants were used as received without further purification. Scheme 2 shows their chemical structures.

2.2 Sample preparation

The sample preparation has been previously reported [27]. For the neat epoxy DGEBA and the hardener 1,2-DCH were initially mixed in a stochiometric ratio of 2:1. For the composites the amount of hardener was adjusted for each concentration of ether-terminated PDMS (up to 15%), the formulations are listed in Table 1. All reactants were mixed at 40°C, first mixing the epoxy and hardener, and then adding the PDMS until a homogeneous mixture was obtained, poured onto molds and then cured at 90°C for 180 min.

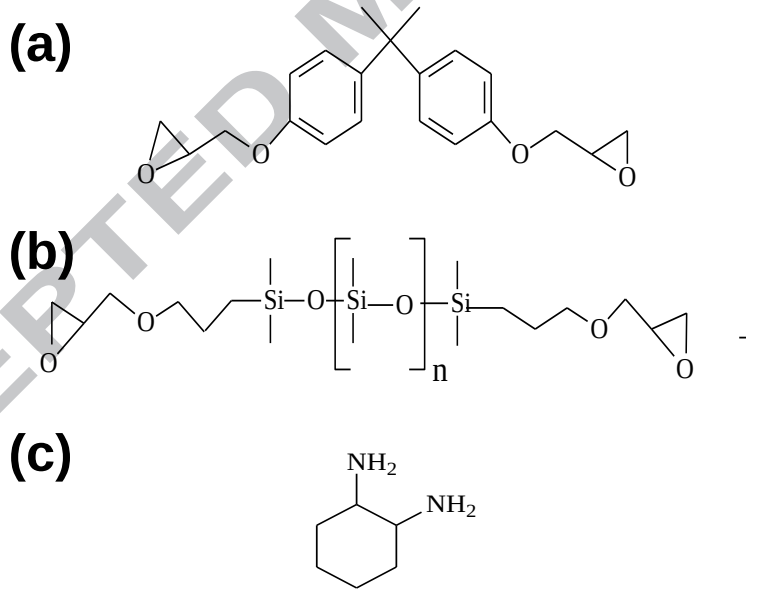

Scheme 2. Chemical structure of (a) diglycidyl ether of bisphenol-A (DGEBA), (b) poly(dimethyl siloxane) diglycidyl ether terminated (PDMS-DGE), and (c) 2-diaminocyclohexane (1,2-DCH).

Table 1. Recipe for DGEBA-PDMS composites.

PDMS (wt%)	DGEBA (g)	1,2-DCH (g)	PDMS-DGE (g)
0	6.8076	1.1727	0
5	6.8090	1.1645	0.3995
10	6.8092	1.2008	0.7960
15	6.8032	1.2772	1.2026

2.3 Thermal analysis

The thermal decomposition temperatures, T_{dec}, were determined by modulated thermogravimetric analysis (MTGA), coupled to high-resolution mode, using the TGA Q5000ir manufactured by TA Instruments (New Castle, DE, USA) under dry nitrogen atmosphere. Samples of about 20 mg were scanned from room temperature at 5°C/min, modulating ± 4°C using 30 seconds period. The thermal transitions were determined by differential scanning calorimetry (DSC) using the Q200™ calorimeter manufactured by TA Instruments (New Castle, DE, USA). Temperature and enthalpy calibration were carried out using analytical grade indium (T_m = 156.6 °C). The thermal transitions were determined at a heating rate of 10 °C/min under dry nitrogen atmosphere.

2.4 Mechanical properties

The flexural elastic modulus and stress at fracture were determined in flexural mode at room temperature using the solids analyzer RSA G2 (TA Instruments, New Castle DE, USA)

and three-point bending mode according to ASTM D-790. The specimen dimension was 25 mm x 3 mm x 1.3 mm. The average value was recorded by testing at least three specimens.

2.5 Hardness

Hardness of epoxy composites were evaluated by conventional *Vickers indentation* measurements. The tests were carried out at room temperature using a HMV Micro Hardness Tester 2.0 (Shimadzu, Kyoto, Japan) equipped with a Vickers indenter. This test uses a square pyramid of diamond with angles α between non-adjacent faces of the pyramid of 136° and the Vickers hardness *HV* was determined by

$$HV = \frac{2 \cdot P \cdot \sin(\alpha / 2)}{d^2} = 1.854 \cdot 10^6 \frac{P}{d^2} \quad (1)$$

where P is the force in Newtons and d is the mean diagonal length of the impression in millimeters [30]. *HV* is then expressed in MPa. Sections of 3 cm x 0.5 cm about 0.2 cm were subjected to a load P of 0.25 N for 6 sec. Each sample was tested at least on five random locations following this protocol and the results are the average of these measurements.

2.6 Morphology

The morphology of the composites was investigated by scanning electron microscopy (SEM) utilizing the VEGA3 SBU (TESCAN, Brno, Czech Republic). Energy dispersive spectroscopy (EDS) was utilized for elemental mapping using an EDS detector XFlash™ 410 M, manufactured by Bruker (MA, USA). Images were obtained in high vacuum mode at 20 kV. EDS spectra and elemental maps were obtained at 20 KV and < 2.5 kcps. Prior to SEM analysis the specimens were gold coated using the SPI Module sputter coater manufactured by SPI Supplies (West Chester PA, USA). The images were analyzed with the software ImageJ [31].

2.7 Contact Angle Measurements

Contact angle measurements of the epoxies were conducted with an in-house built instrument utilizing an optical microscope Stereomaster II, Fisher Scientific Model SPT-ITH equipped with a Motic1000 digital camera (Motic, China) and sand blasted glass (Edmunds Optics) [32]. The volume of the drop was maintained at 10 μL in all cases using a microsyringe. Measurements were repeated 5 times on different regions of the same sample.

3. Results and discussion

3.1 Thermal properties

The kinetics of curing of DGEBA-PDMS composites with 5 wt% ether-terminated PDMS content was investigated over a range of temperatures (90 to 140°C) and has been reported elsewhere [27]. In this research composites where the PDMS content was varied up to 15 wt% and cured at 90 °C for 180 minutes were investigated. The thermal stability of the composites thus obtained was determined via thermogravimetric analysis, TGA, using modulated mode and high resolution. Figure 1 shows mass loss traces as a function of temperature for DGEBA-PDMS composites with (a) 0, (b) 5, (c) 10, and (d) 15 wt% PDMS content. The results show that neat DGEBA (Figure 1(a)) exhibit a 5 % mass loss at T_{dec} =287.9°C.

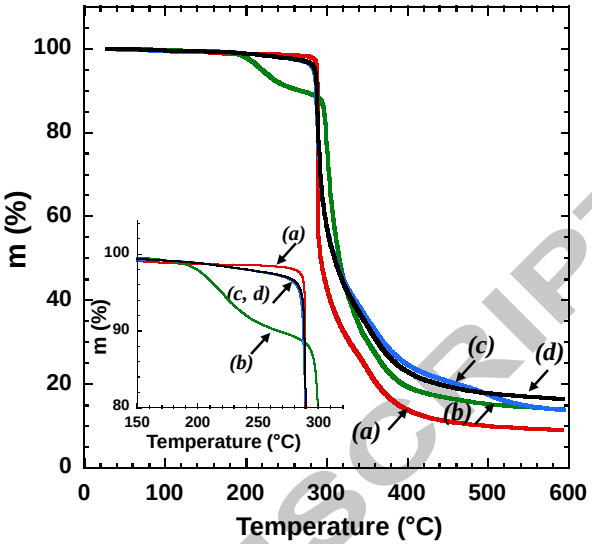

Figure 1. Plot of mass loss as a function of temperature of DGEBA/PDMS composites containing (a) 0, (b) 5, (c) 10, and (d) 15 wt% PDMS.

Increasing temperature there is a sudden mass loss up to about 300°C where the rate of mass loss slowed down, decaying gradually, and by 520°C all material has burnt up and mass loss has reached a plateau. The composites with 5wt% PDMS (Figure 1(b)) exhibited an onset of mass loss at ca. 195°C. This composite lost about 10 % mass before reaching a second onset of thermal decomposition temperature at T_{dec} =297°C, as clearly shown in the inset of Figure 1. The increase of concentration of PDMS up to 15 wt% did not increase the thermal decomposition temperature but rather T_{dec} slightly decreased relative to the neat epoxy resin. After the onset of thermal decomposition the nanocomposites initially exhibited a rapid mass loss, and afterwards the rate of mass loss was slower than the neat resin. It is suggested that at 5 wt% concentration the siloxane phase is better dispersed in the epoxy matrix and acting as "protective layer" of the epoxy matrix thus rendering higher thermal stability. However, it is unclear why the 5 wt% composite exhibit thermal decomposition at lower temperature. Experiments have been repeated for freshly cured specimens and the results are reproducible. In order to better understand this behavior more TGA investigation is being carried out for a range of compositions around 5 wt%.

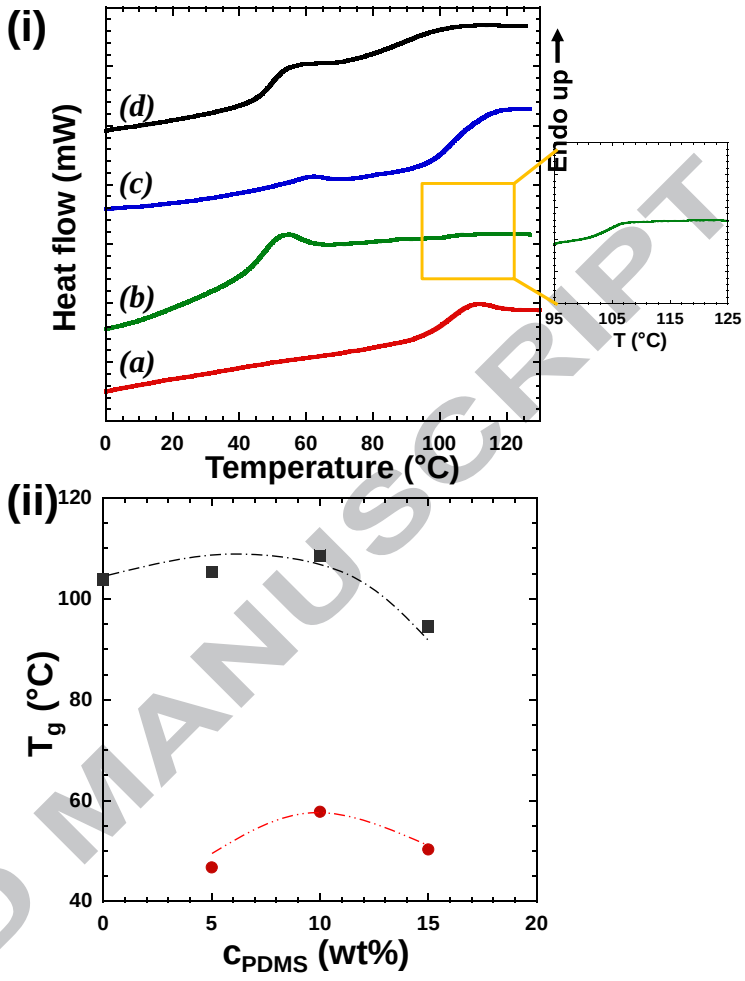

Figure 2. (i) DSC heating scans of DGEBA/PDMS composites containing (a) 0, (b) 5, (c) 10, and (d) 15 wt% PDMS. (ii) Glass transition temperatures T_g as a function of PDMS content. Inset shows weak high temperature T_g for the 5 wt% composite.

Modulated TGA also enabled the determination of the activation energy for thermal decomposition for each sample, and these are listed in Table 2.

The influence of the rubbery phase on the thermal transitions of the composites was investigated by DSC, Figure 2(i) shows heating scans of the as-cured composites. The neat epoxy (trace a) exhibits a glass transition temperature T_g at ca. 103 °C. Strikingly, the composites with 5 and 10 wt% PDMS content (traces b and c) exhibit two glass transitions, a low temperature T_g in the range of 50-60 °C, and a high temperature T_g at ca. 105-108 °C. Further increase of PDMS content decreased the high temperature T_g (trace d). The behavior of glass

transition temperatures as a function of PDMS concentration is clearly appreciated in Figure 2(ii); the thermal properties are summarized in Table 2.

Table 2. Thermal properties of DGEBA-PDMS composites

c_{PDMS} (wt%)	T_g (°C)	T_{dec} (°C)	$E_{a,dec}$ (KJ/mol)
0	103.9	287	185
5	46.8	198.3	252
	105.4	296.9	88
10	57.1	285.4	164
	108.6		
15	50.3	287.2	140
	94.6		

The higher glass transition temperatures for the 5 and 10 wt% composites could be rationalized as follows: dissolution of PDMS into the epoxy matrix should decrease its T_g (plasticization effect). However, Figure 2ii and Table 2 show a slight increase in the T_g of the matrix (the highest T_g) for formulations containing 5 and 10 wt % PDMS. Apart from the micrometric phase separation, there should be a secondary phase separation of nanometric PDMS/epoxy interpenetrated domains with a T_g lower than the neat matrix (see section 3.4, in particular Figure 11b, where it shows a uniform distribution of siloxane phase throughout the epoxy matrix). The increase in crosslink density produced by these domains could explain the slight increase in the T_g of the epoxy matrix devoid of PDMS.

On the other hand, the low glass transition temperatures (~50°C) suggest some interactions and degree of interpenetration of the ether-terminated PDMS into the epoxy phase. That is, it is suggested that this functional PDMS disrupted/interpenetrated to some extent the epoxy phase, a result observed in epoxy resins blended with polymers with different functionalities, epoxy-rubbers and epoxy-thermoplastics blends [33, 34]. Phase separation of PDMS takes place during cure thus generating heterogeneity, and hence a very low content would be enough for toughening (as shown in section 3.2). Furthermore, it is believed that the oxirane functionality of PDMS permits to form covalent interactions at the epoxy interface giving rise to the low temperature T_g. The low temperature T_g upon addition of PDMS would arise from the incomplete phase separation caused by plasticization phenomenon, i.e., a degree of interpenetration between phases, that has been reported in several rubber modified epoxy formulations [11, 33, 35]. These covalent interactions would be reflected in the mechanical properties of these composites, as shown below. The low temperature phase transition of PDMS was investigated by dynamic mechanical analysis (DMA) by carrying out dynamic temperature ramps from -140°C. However, it was found that the glassy modulus of the epoxy phase (>3 GPa) overwhelms any possible signal arising from PDMS, especially so as we are using low concentrations of PDMS. However, the influence of the rubbery phase is manifested in the higher temperature range (above room temperature) due to the macromolecular mobility of the epoxy phase. The dynamic mechanical properties of the composites will be reported elsewhere.

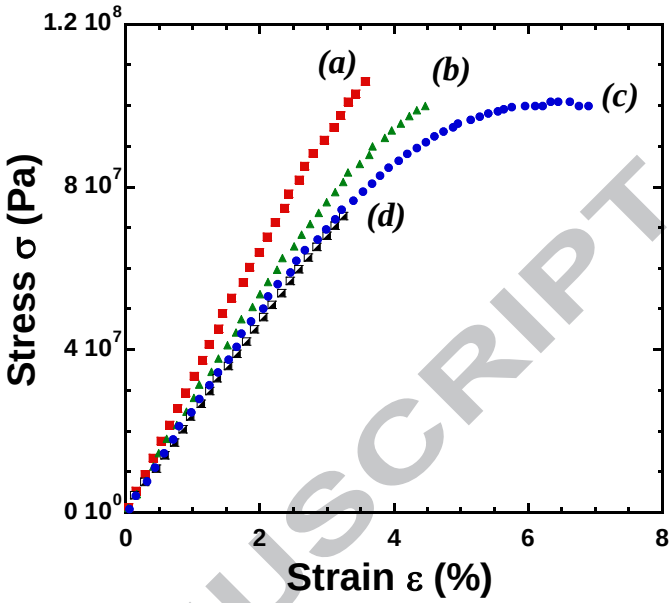

Figure 3. Flexural stress-strain traces of DGEBA/PDMS composites containing (a) 0, (b) 5, (c) 10, and (d) 15 wt% PDMS, at room temperature.

3.2 Mechanical properties

The mechanical behavior of the epoxy-siloxane composites was investigated via flexural deformation, at room temperature. Figure 3 shows the stress-strain traces of DGEBA-PDMS with (a) 0, (b) 5, (c) 10, and (d) 15 wt% PDMS content. The traces correspond to the average of at least three tests on each sample. The trace of the neat epoxy exhibits linear, elastic regime up to about 1.5% strain and fractured at about 3.5% strain. Strikingly, the composites (traces b-d) exhibited considerable more flexural deformation than DGEBA, at 5 wt% the strain at fractured increased up to 5% and at 10 wt% the strain at fractured reached ca. 7%, i.e., a twofold increase relative to the neat epoxy. Further increase of PDMS concentration up to 15 wt% did not increase the strain at fracture, but actually decreased relative to the neat epoxy resin.

The Young's modulus was extracted from the elastic regime of the stress-strain curves, and it was found to be a decreasing function of PDMS content, these values are summarized in Table 2. Furthermore, from the area under the stress-strain traces the toughness was determined and the results are also summarized in Table 3. Note that with 5wt% PDMS the composite

exhibited a modest increase in toughness relative to the neat epoxy. However, at 10 wt% PDMS content the toughness increased twofold. Further increase of PDMS content did not increase toughness, but it actually significantly decreased. It is suggested that the high concentration of PDMS droplets in the epoxy matrix induced defects thus compromising the flexural mechanical properties. This will be further discussed in light of the morphology analysis in section 3.4. The stress and strain at fracture (σ_f, ε_f) for all composites are listed in Table 3.

The flexural stress-strain behavior of these composites shown in Figure 3 mimics the behavior reported for the nanocomposite counterparts [28, 29]. However, the DGEBA-PDMS nanocomposites exhibited considerable more strain at fracture and toughness, denoting the degree of interaction/interpenetration at the nanoscale between the siloxane and epoxy phases. For instance, at 5 wt% concentration of PDMS the nanocomposites exhibited over 9% strain at fracture and toughness of 450 KJ/m^3, nearly twofold increase relative to the composite at the same PDMS content [29]. The increase and then decrease of toughness with rubber content has also been reported for an epoxy-natural rubber composite [36]. It is noted that the critical stress intensity factor would be a better measurement of toughness. However, the area under the stress-strain curve is also an acceptable and widely used measurement of toughness, see Gleghorn et. al. (2008) [37] and references therein.

Table 3. Mechanical properties of DGEBA-PDMS composites.

c_{PDMS} (wt.%)	E (GPa)	σ_f (MPa)	ε_f (%)	Toughness (kJ/m^3)
0	3.3±0.12	106±8	3.5±0.5	200±18

5	2.8±0.16	100±12	4.4±0.6	252±24
10	2.5±0.15	100±18	6.9±0.9	470±36
15	2.3±0.21	75±9	3.3±0.6	125±16

Hardness measurements, Vickers type, of the composites, *HV*, at room temperature were attempted using micro-indentation. During the course of the measurements it was noticed that upon releasing the weight the indentations exhibited some elastic recovery. Moreover, for the composite with 15 wt% PDMS content the indentations nearly disappeared after few minutes. The partial elastic recovery of the indentations gave rise to unreasonably high hardness values. Therefore, the partial recovery of the indentations prevented reliable hardness measurements, at least at the conditions utilized in this research.

3.3 Wetting behavior

Water contact angle measurements were carried out on all DGEBA-PDMS composites, and photographs of water droplets on the specimens' surfaces are shown in Figure 4(a-d). The neat DGEBA epoxy displayed a water contact angle of 78°, Figure 4(a), in agreement with previous reports [27-29]. At 5 wt% PDMS content the contact angle increased up to 89°. It is noted that the contact angles are accurate within ±3° based on 10 independent measurements for each specimen. Figure 4 shows that at 10 and 15 wt% PDMS content the contact angle decreased even below that for the neat epoxy resin. Then, it appears that there is an optimum concentration of PDMS between 5 and 10 wt% for slightly hydrophobic behavior of these composites, as shown in Figure 4(e).

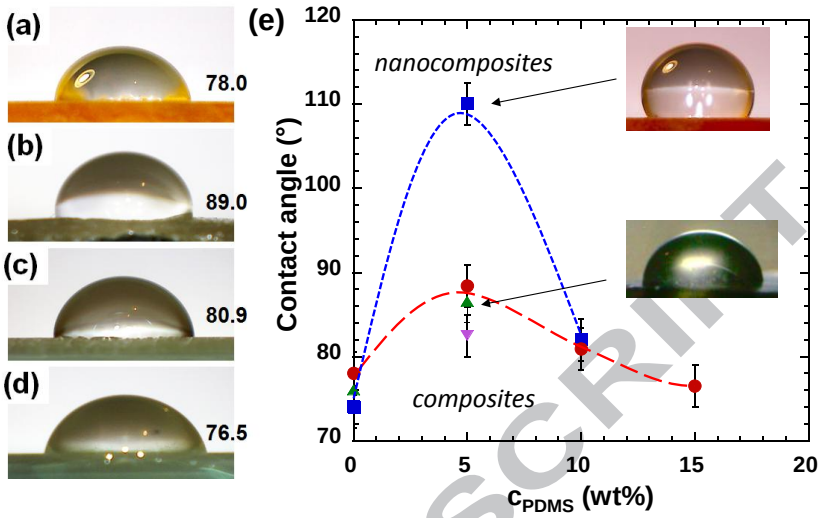

Figure 4. Water droplets on DGEBA/PDMS composites as a function of PDMS concentration: (a) 0, (b) 5, (c) 10, and (d) 15 wt%. Contact angles (±3°) are indicated. (e) Plot of contact angle as a function of PDMS concentration (●). Data for equivalent nanocomposites (■) [28, 29] and composites cured at 95°C (▲) and 100°C (▼) are included [27].

These results are distinctly different to those obtained with the DGEBA-PDMS *nanocomposites*.[28, 29] For instance, the water contact angle was as high as 110° for the nanocomposite with 5 wt% PDMS concentration, as shown in Figure 4(e). However, it is noted that the contact angle was then reduced to only 82° when increasing the concentration of PDMS up to 10 wt%, quite similar to the values obtained with the composite counterpart, Figure 4(e). A reduction of contact angle has also been observed when increasing curing temperature of the DGEBA-PDMS composites (filled triangles in Figure 4e) [27]. AFM measurements on the composites were carried out and found an increase and then a reduction of roughness when increasing the concentration of PDMS (see section 3.4). This may be the reason for the contact angle reduction in the composites. The significantly higher contact angle found for the nanocomposite with 5 wt% PDMS was also attributed to the well dispersed PDMS nanodomains in the epoxy matrix [29]. AFM measurements remain to be carried out on the nanocomposites. However, it is recognized that more research needs to be done to better understand the wetting behavior in DGEBA-PDMS composites *and* nanocomposites.

3.4 Morphology

The fractured specimens were examined using scanning electron microscopy (SEM) in order to better understand the mechanical behavior of these composites. Figure 5 shows a SEM micrograph and EDS maps and spectrum of a fractured surface of the neat epoxy resin DGEBA cured at 90°C. The micrograph shows that the fractured surface exhibits sharp edges and fan morphology, typical of brittle mechanical behavior.

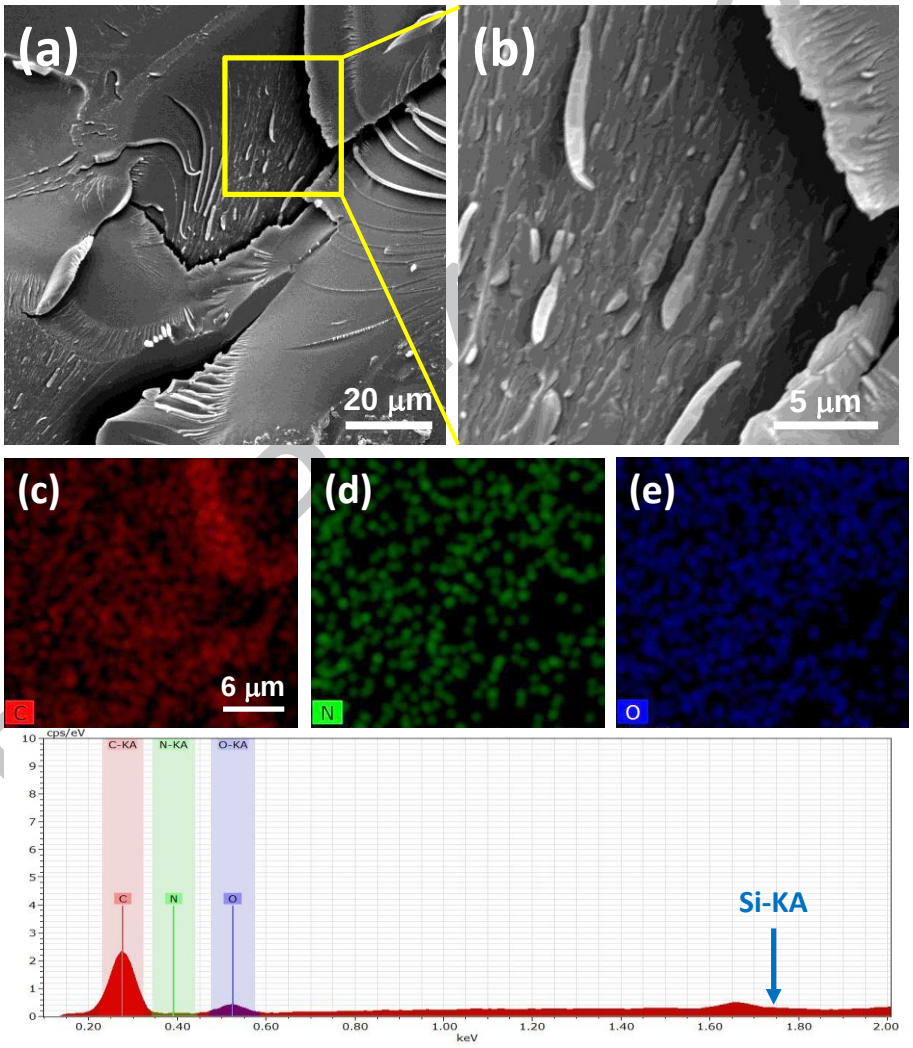

Figure 5. SEM micrographs and corresponding EDS elemental maps and X-ray spectrum of a fractured surface of DGEBA epoxy resin.

The Figure 6(a) shows SEM a micrograph of the fractured surface of the composite DGEBA-PDMS 5wt%. Figure 6(b) shows a higher magnification evidencing the homogeneous dispersion of micro droplets. A number of micrographs were analyzed to build a histogram of droplet diameter for this composite; the size distribution is shown in Figure 6(c). The size distribution is bimodal and the mean diameter was found to be 0.78 μm. A smaller population of smaller droplet diameter about 0.3 μm was also detected.

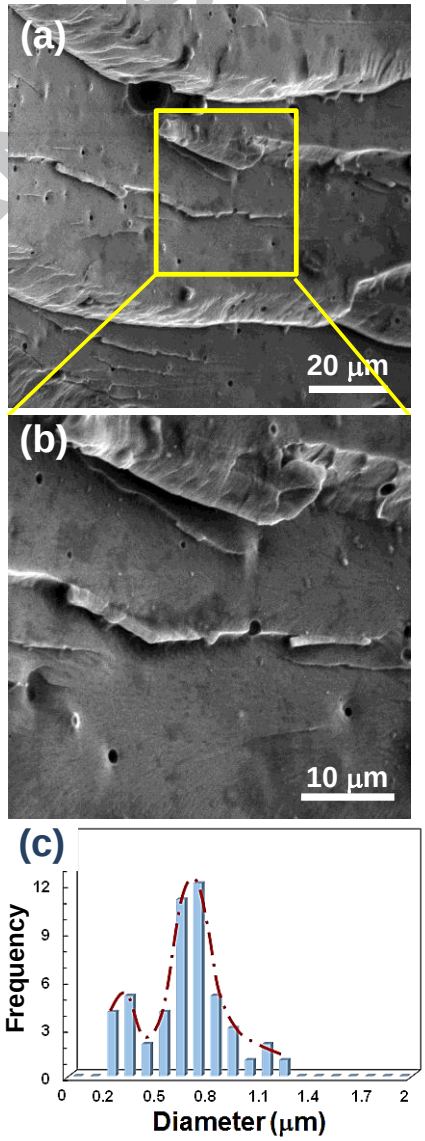

Figure 6. (a, b) SEM micrographs of fractured surface of DGEBA-PDMS composite with 5 wt% PDMS concentration. (c) Histogram of PDMS droplets diameter.

The SEM micrographs show that the composite still exhibits brittle fracture despite smaller Young's modulus and greater toughness than the neat epoxy resin. The rather small PDMS droplet sizes are consistent with a previous study [27], suggesting the oxirane end groups of PDMS indeed contributed to reduce the DGEBA-PDMS phase separation during curing.

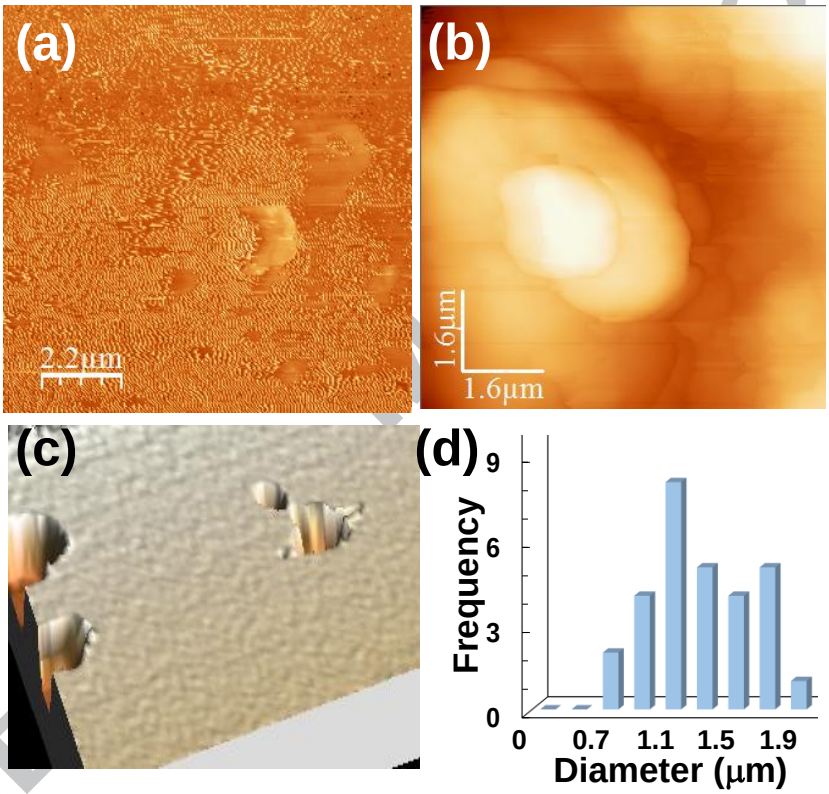

Figure 7. AFM micrographs of DGEBA-PDMS composites with: (a) 0, and (b) 5 wt% PDMS content. (c) AFM micrograph of fractured surface of the 5 wt% composite. (d) Histogram of droplet diameters determined from AFM micrographs.

As the composites morphology exhibit craters and pits, the composites were also examined by atomic force microscopy (AFM) in order to better assess the droplet morphology and the droplet sizes. Figure 7 shows a series of AFM micrographs of the surface of (a) the neat

epoxy and (b) the 5 wt% composite. The droplet morphology is apparent in this micrograph. Figure 7(c) shows the micrograph of a fractured surface of the composite, this clearly enables to better assess the size of the droplets. Figure 7(d) shows the histogram of droplet diameters determined from AFM micrographs. The results showed a mean droplet diameter of 1.3 μm, the same order of magnitude but slightly larger than values obtained from the analysis of SEM micrographs. The roughness was also determined using AFM and the RMS roughness for the neat epoxy was 9 (±2) nm. On the other hand, the RMS roughness for the 5 wt% composite was significantly increased up to 18 (±4) nm.

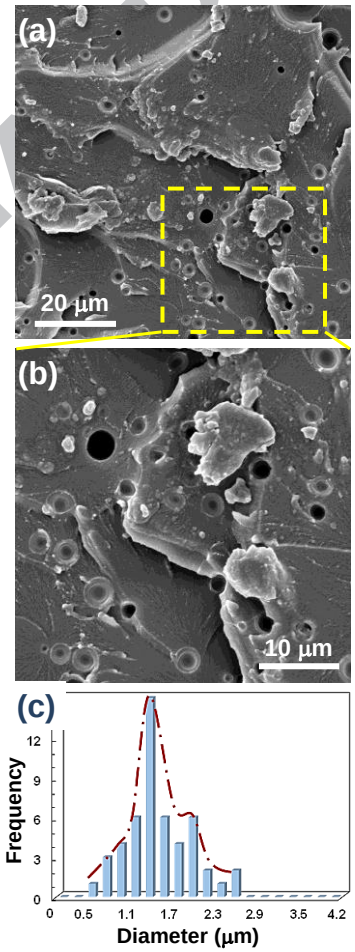

Figure 8. (a, b) SEM micrographs of fractured surface of DGEBA-PDMS composite with 10 wt% PDMS concentration. (c) Histogram of droplets diameter.

Figure 8(a, b) shows SEM micrographs of the fractured surface of DGEBA-PDMS composite with 10 wt% PDMS content. The morphology exhibits sharp edges in the epoxy

matrix and uniform distribution of droplets. These results suggest that the composite suffered brittle fracture. Examination of the PDMS droplet morphology at higher magnification shown in Figure 8(b) clearly identifies two types of failure. There are rather few empty circular cavities where the PDMS phase was pulled off the epoxy matrix during fracture. This morphology would suggest no interaction between the siloxane and epoxy phases. On the other hand, the majority of droplet morphology consists of circular cavities resembling craters. This morphology would arise from incomplete pull off of the PDMS phase, and therefore it suggests strong interaction between the siloxane and epoxy phases. This interaction would explain the much greater toughness of this composite. Figure 8(c) shows the distribution of droplet size of this composite, the mean droplet diameter being 1.51 μm.

Figure 9(a) shows an AFM micrograph of the surface of the 10 wt% composite. The droplet morphology is apparent in this micrograph. Figure 9(b) shows the histogram of droplet diameters determined from AFM micrographs. The results showed a mean droplet diameter of 2.2 μm, this is again of the same order of magnitude but slightly larger than values obtained from the analysis of SEM micrographs (see Figure 8(c)). Interestingly, the roughness of this composite was reduced; it was determined to be 7 (±3) nm. Note that the increase and then decrease of roughness as determined by AFM mimics the behavior of water contact angle (see Figure 4), thus suggesting that roughness drives this phenomenon. However, more research needs to be done on composites cured under different conditions as well as on the equivalent nanocomposites before any conclusions could be drawn.

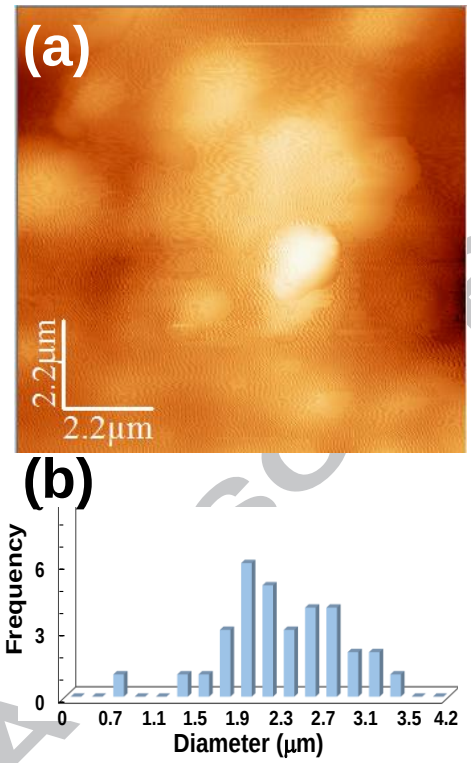

Figure 9. (a) AFM micrograph of DGEBA-PDMS composites with 10 wt% PDMS content. (b) Histogram of droplet diameters determined from AFM micrographs.

The morphology of the composite with 15 wt% concentration of PDMS is shown in Figure 10. The SEM micrographs show a droplet morphology uniformly dispersed indicating that the PDMS phase is well dispersed throughout the epoxy resin.

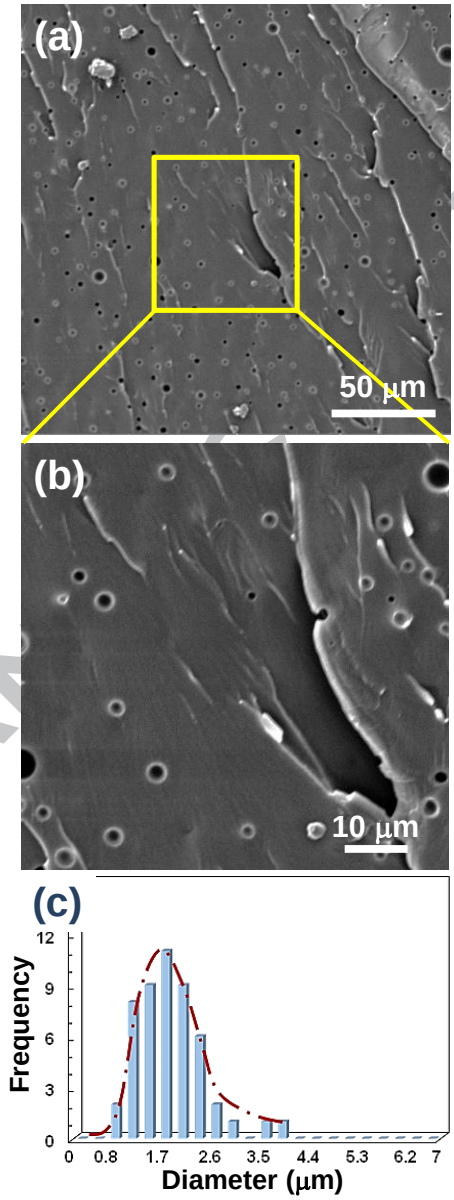

Figure 10. (a, b) SEM micrographs of fractured surface of DGEBA-PDMS composite with 15 wt% PDMS concentration. (c) Histogram of droplets diameter.

The droplet size distribution is shown in Figure 10(c), and the results show that the droplets for the 15 wt% composite have a mean diameter of 1.92 μm. It is noted that the morphology of the fractured surfaces consist of greater population of empty cavities as well as incomplete, crater-like, cavities.

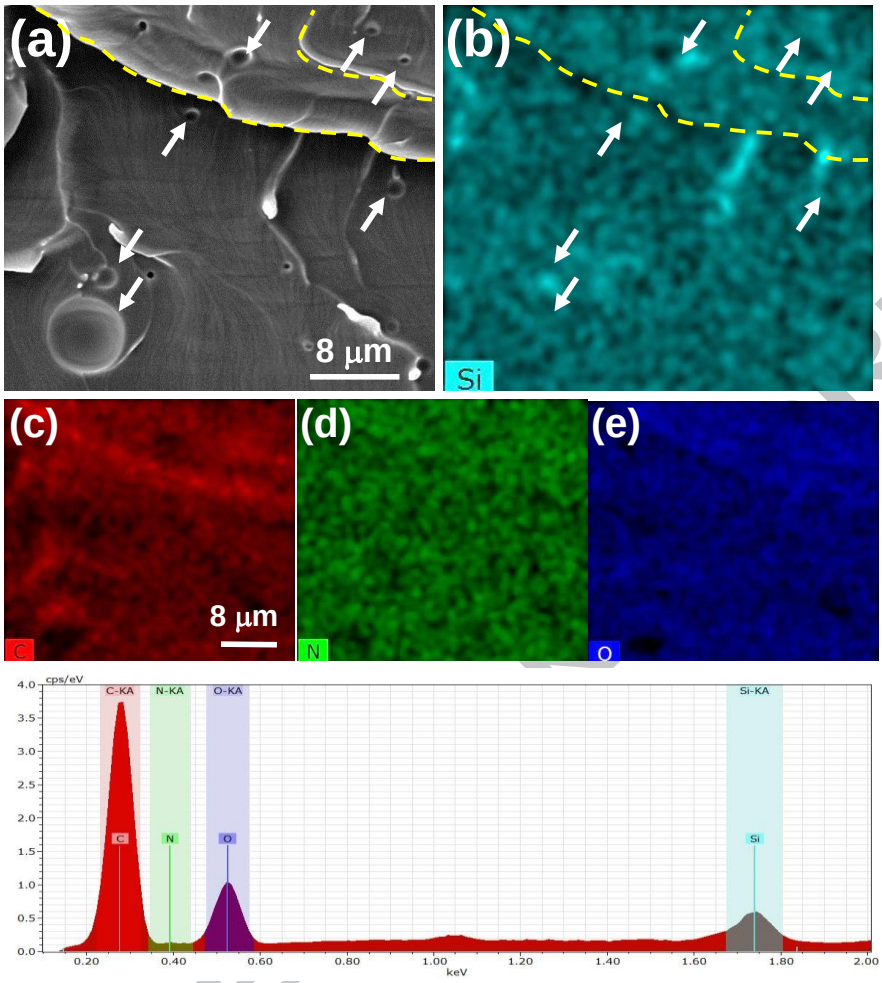

Figure 11. EDS elemental maps and X-ray spectrum of fractured surface of DGEBA-PDMS composite with 5 wt% PDMS concentration.

The question of the possible interaction between DGEBA and PDMS was further investigated by carrying out elemental mapping using EDS analysis of the cavities left after the PDMS phase was pulled off the epoxy matrix, i.e., the crater-like droplet morphology was investigated in detail carrying out EDS analysis. Figure 11(a) shows a higher magnification SEM micrograph, Figure 11(b-e) the corresponding elemental maps, and Figure 11(f) shows the X-ray spectrum of a fractured surface of the DGEBA-PDMS composite with 5 wt% PDMS content. The arrows in Figures 11 (a) and (b) define the location of the cavities created after the PDMS

phase was pulled off the epoxy matrix during fracturing. The *Si* map, shown in Figure 11(b), demonstrates a uniform distribution of siloxane phase throughout the epoxy matrix. Furthermore, the intensity of the *Si* signal is not reduced at the cavities thus suggesting that a fraction of the siloxane phase remained attached to the epoxy matrix after fracturing. It is pointed out that the histogram of droplet diameter shown in Figure 7(c) was determined from a number of SEM micrographs. The higher magnification SEM micrograph shown in Figure 10 exhibits one rather large cavity which is not representative of the overall morphology. This micrograph was only utilized to show the presence of *Si* in the cavities.

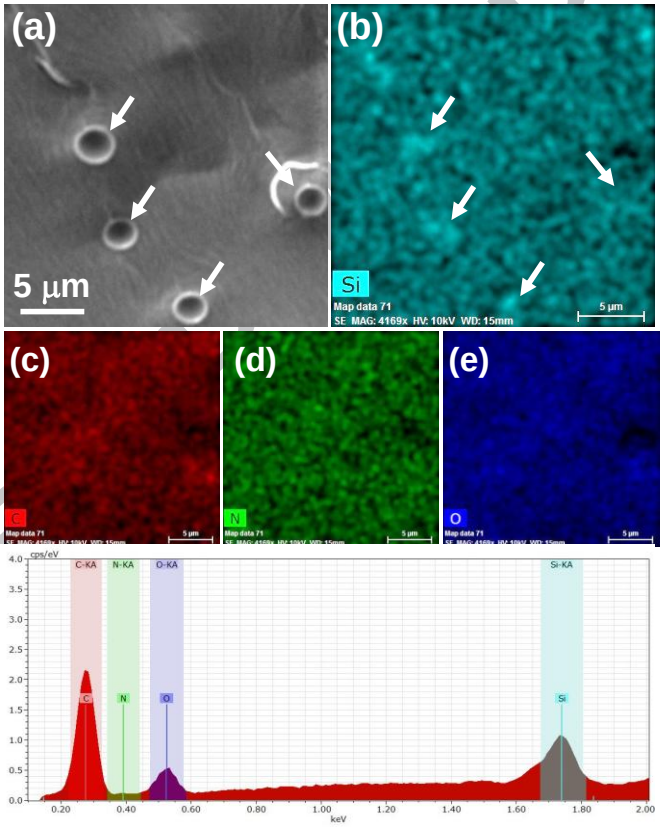

Figure 12. EDS elemental maps and X-ray spectrum of fractured surface of DGEBA-PDMS composite with 10 wt% PDMS concentration.

The detailed analysis of the cavities was also carried out for the DGEBA-PDMS composite with 10 wt% PDMS content, a higher magnification SEM micrograph and corresponding elemental maps and X-ray spectrum are shown in Figure 12. The arrows in Figures 12 (a) and (b) define the location of the cavities created after the PDMS phase was pulled off the epoxy matrix during fracturing. The *Si* map clearly shows that the composite contains a relatively uniform distribution of siloxane throughout the epoxy matrix. Strikingly, the *Si* signal is stronger at the cavities suggesting therefore higher concentration of siloxane phase and confirming that during fracture a layer of siloxane was left behind. The X-ray spectrum also shows that the signal of the Si-Kα peak is also stronger (relative to C and O peaks) due to the higher concentration of *Si* in the composite.

The partial miscibility of the ether terminated PDMS into the epoxy resin indicated by the DCS results would suggest that some fraction of PDMS was incorporated into the crosslinked network. It is considered that this system cannot be treated as a particulate filled epoxy composite. To test this hypothesis the Young's modulus was fitted using Phillips model [38] which has been shown to work well for preformed silicone rubber particles dispersed in an epoxy resin [39].

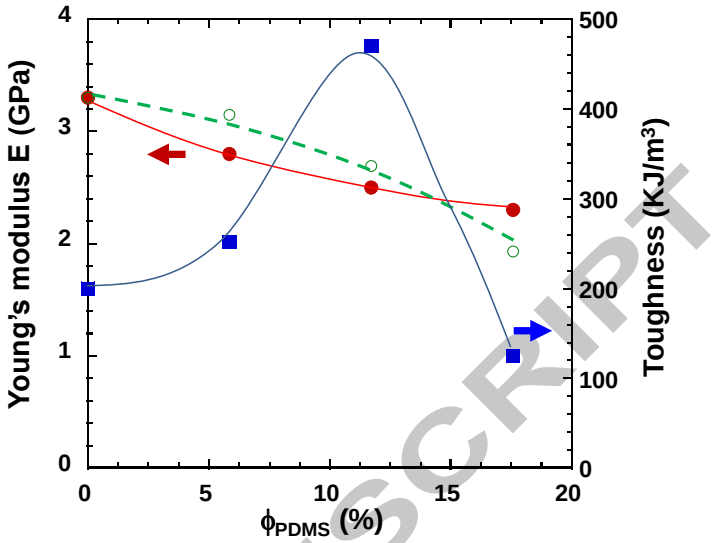

Figure 13. Young's modulus and toughness as a function of volume fraction of PDMS. Open circles and dotted line corresponds to values calculated by Phillips model [38], equation 2.

Phillips [38] suggested the following expression for the Young's modulus of micrometer scale particles reinforced composites assuming a simple model based on a cubic array of equivalent volume fraction to spherical particles dispersed in a continuous phase

$$\frac{E_c}{E_m} = \frac{X^2}{1 - X \cdot (1 - E_m / E_f)} + (1 - X^2) \qquad (2)$$

where E_c, E_m and E_f are the Young's moduli of the composite, the matrix and the microfiller, respectively. X is related to the volume fraction of the microfiller, ϕ_f, by

$$X = (P \cdot \phi_f)^{1/3} \qquad (3)$$

where P is a disposable parameter described as "relative volume fraction" since it is the ratio of volume of equivalent cubic particles/volume of spherical particles. For spherical particles P=1.91 and $2/\sqrt{3} \cdot \pi$=0.37 for the upper and lower bound, respectively. The results are shown in Figure 13. The dotted line corresponds to Young's modulus values calculated by equation 2 and using E_f =3 MPa [39] and P=0.11. Note that Phillips model does a reasonable job, however the value of P is below the lower limit of spherical particles suggesting therefore that the model is not adequate for our system. This may be due to the interpenetrated nature of the composite.

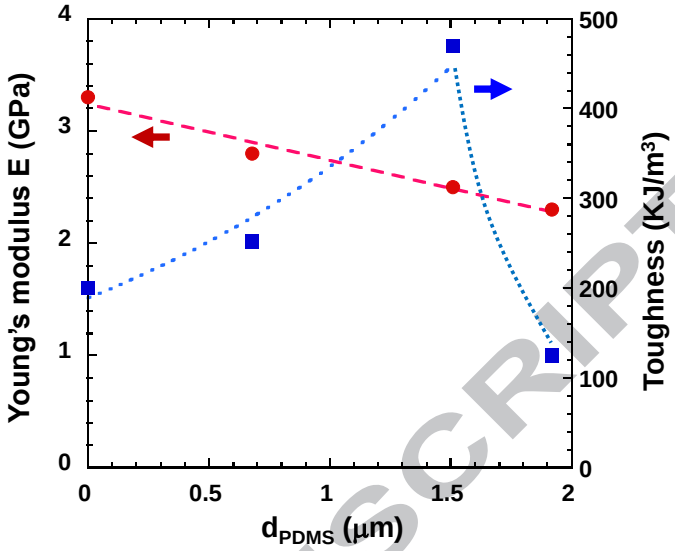

Figure 14. Young's modulus and toughness as a function of PDMS average droplet size (as determined by SEM). Dotted lines correspond to linear and exponential data fit, respectively.

The mechanical properties however were found to obey simple scaling relationships with PDMS' average droplet size (as determined by SEM), as shown in Figure 14. These results show that the composite Young's modulus obeys a linear relation, and the best fit to experimental data gives

$$E_c = 3.24 - \frac{1}{2} \cdot d_{PDMS} \qquad (4)$$

with fit factor r=0.98. It was verified that the same scaling applies when using diameter values obtained by AFM. On the other hand, the composite's toughness appears to follow an exponential growth up to 10 wt% PDMS content. However, at 15 wt% concentration the toughness drops drastically reflecting the influence of the soft rubbery phase, a behavior typical of epoxy/rubber composites [40-42].

The results of this investigation showed that ether-terminated PDMS is effective to enhance strain at fracture and toughness in DGEBA epoxy resin. These mechanical properties showed a maximum at ca. 10 wt% PDMS content. The method to produce these composites is simple as it only involves the direct mixing of PDMS with DGEBA and the curing agent, DCH. The critical concentration found in this research is similar to that identified for functional rubber

modified epoxy resin composites. For instance, Barcia et al [40] showed that the impact strength of hydroxyl terminated polybutadiene (HTPB), first functionalized with a silane, was optimum at ca. 10% concentration. A pre-step was involved as HTPB was first reacted with toluene di-isocyanate (TDI) to enhance the compatibility with the epoxy resin. Similarly, Matthew et al [41] showed that epoxidized natural rubber (ENR) increased the fracture toughness of epoxy, reaching a maximum at ca. 10 wt % concentration. The droplet size, however, ranged from ca. 2 to 5 μm. On the other hand, Thomas et al [42] reported an optimum concentration of 15 wt% for maximum impact strength of carboxyl-terminated poly(butadiene-co-acrylonitrile) (CTBN) / epoxy blends. The size of the precipitated rubber ranged from 0.8 to 1.4 μm. Although partial miscibility of PDMS into the epoxy matrix was present, as evidenced by a lower temperature glass transition, at 10 wt% PDMS content the flexural modulus only decreased by ca. 25%, but toughness and strain at fracture increased ca. 200%, relative to the neat epoxy.

The mechanical behavior of these composites is distinctly different, actually inferior to that reported in its nanocomposite counterparts [28, 29]. The DGEBA-PDMS *nanocomposites* exhibited droplet size ca. 250 nm and an optimum concentration of PDMS of 5 wt%, where strain at fracture and toughness increased up to 300%.

Further insight into the reinforcing mechanism of ether terminated PDMS would arise from the kinetics of droplet formation and dynamic mechanical properties of these composites. These have been investigated and will be reported elsewhere.

4. Conclusions

This research has shown that the addition of ether-terminated PDMS to DGEBA epoxy was effective to produce composites with enhanced toughness and strain at fracture; toughness

increased twofold at only 10 wt% PDMS content. PDMS and DGEBA phase separated during curing forming droplet morphology. However, the phase separation was greatly hindered by the functional end groups of PDMS thus producing droplets with sizes ranging from 0.6 μm to 1.8 μm. Furthermore, there was some degree of interpenetration of the siloxane phase into the epoxy network. The composites exhibited a high glass transition temperature, T_g, around 103°C, with a slight increase of T_g for formulations containing 5 and 10 wt % PDMS, and a lower T_g ca. 50°C. The unusual higher T_g suggests a secondary phase separation of nanometric PDMS/epoxy interpenetrated domains with a T_g lower than the neat matrix. The increase in crosslink density produced by these domains could explain the slight increase in the T_g of the epoxy matrix devoid of PDMS. The dispersed siloxane phase also initially produced an increase and then a decrease of toughness as PDMS content increased. The mechanical modulus was found to decrease with linear scaling with droplet size, as determined from SEM micrographs. The results of this investigation suggest that utilization of functional PDMS is a good approach to produce epoxy composites with enhanced flexural properties thus opening up opportunities in diverse applications as electronic coatings and structural applications.

Symbols and Abbreviations

AFM	atomic force microscopy
DGEBA	diglycidyl ether of bisphenol-A
PDMS-DGE	poly(dimethyl siloxane) diglycidyl ether terminated
1,2-DCH	1,2-diaminocyclohexane
DSC	differential scanning calorimetry
E	Young's elastic modulus

$E_{a,dec}$	activation energy for thermal degradation
EDS	Energy dispersive spectroscopy
SEM	Scanning electron microscopy
T_g	glass transition temperature
TGA	Thermogravimetric analysis
T_{dec}	thermal degradation temperature
σ	stress
ε	strain

Acknowledgement

Thanks to L.G. Reyes-Mayer for help with water contact angle measurements. The SEM/EDS was funded by the Mexican Council for Science and Technology (CONACyT) under the Apoyo al Fortalecimiento y Desarrollo de la Infraestructura Científica y Tecnológica Convocatoria 2015 program, grant 254458. The authors thank the anonymous reviewers; their observations greatly benefited the manuscript.

References

1. Lee H, Neville C. Epoxy resins: their applications and technology. McGraw Hill: New York; 1957.
2. May CA. Epoxy Resins Chemistry and Technology, 2nd ed., Marcel Dekker ed, Inc.: New York; 1988.

3. Laza JM, Julian CA, Larrauri E, Rodríguez M, León LM. Thermal scanning rheometer analysis of curing kinetic of an epoxy resin: 2. An amine as curing agent. Polymer 1999; 40: 35-45.
4. Carrozzino S, Levita G, Rolla P, Tombari E. Calorimetric and microwave dielectric monitoring of epoxy resin cure. Polymer Eng Sci 1990; 30: 366-373.
5. Vyazovkin, S, Sbirrazzuoli N. Mechanism and Kinetics of Epoxy-Amine Cure Studied by Differential Scanning Calorimetry. Macromolecules 1996; 29: 1867-1873.
6. Bucknall CB. Toughened Plastics. Applied Science: London; 1977.
7. Sultan JN, McGarry FJ. Effect of rubber particle size on deformation mechanisms in glassy epoxy. J Polym Eng Sci 1973; 13: 29-34.
8. McGarry FJ, Rosner RB. Epoxy Rubber Interactions. In: Riew CK, Kinloch AJ. eds. Toughened Plastics I. Science and Engineering. Advances in Chemistry Series: Washington, DC; 1993. 305-315
9. McGarry FJ. In Polymer Toughening, Arends CB. ed. Marcel Dekker, Inc.: New York; 1996. pp 175-188.
10. Parameswaranpillai J, Woo EM, Hameed N, Piontek J eds. *Handbook of epoxy blends*, Springer, Switzerland, 2015
11. Robenson LM. *Polymer Blends: A Comprehensive Review*. Carl Hanser Verlag GmbH & Co: Munich; 2007.
12. Chikhi N, Fellahi S, Bakar M. Modification of epoxy resin using reactive liquid (ATBN) rubber. European Polym J 2002; 38: 251-264.
13. Ramos VD, Da Costa HM, Soares VLP, Nascimento RSV. Modification of epoxy resin: a comparison of different types of elastomers. Polymer Testing 2005; 24: 387-394.

14. Tripathi G, Srivastava D. Effect of carboxyl-terminated poly(butadiene-co-acrylonitrile) (CTBN) concentration on thermal and mechanical properties of binary blends of diglycidyl ether of bisphenol-A (DGEBA) epoxy resin. Mat Sci Eng A 2007; 443: 262-269.
15. Thomas R, Yumei D, Yuelong H, Le Y, Moldenaers P, Weimin Y, Czigany T, Thomas S. Miscibility, morphology, thermal and mechanical properties of a DGEBA based epoxy resin toughened with a liquid rubber. Polymer 2008; 49: 278-294.
16. Thomas R, Durix S, Sinturel C, Omonov T, Goossens S, Groeninckx G, Moldenaers P, Thomas S. Cure kinetics, morphology, and miscibility of modified DGEBA-based epoxy resin – Effects of a liquid rubber inclusion. Polymer 2007; 48: 1695-1710.
17. Calabrese L, Valenza A. Effect of CTBN rubber inclusions on the curing kinetic of DGEBA-DGEBF epoxy resin. European Polym. J. 2003; 39: 1355-1363.
18. Xu F, Du X-S, Liu H-Y, Guo W-G, Mai Y-W. Temperature effect on nano-rubber toughening in epoxy and epoxy/carbon fiber laminated composites. Composites B 2016; 95: 423-432
19. Chrusciel JJ, Lesniak E. Modification of epoxy resins with functional silanes, polysiloxanes, silsesquioxanes, silica and silicates. Prog. Polym. Sci. 2015; 41: 67-121.
20. Zhao F, Sun Q, Fang DP, Yao K. Preparation and Properties of Polydimethylsiloxane-Modified epoxy Resins. J. Appl. Polym. Sci. 2000; 76: 1683-1690.
21. Hou SS, Chung YP, Chan CK, Kuo PL. Function and performance of silicone copolymer. Part IV. Curing behavior and characterization of epoxy-siloxane copolymers blended with diglycidyl ether of bisphenol-A. Polymer 2000; 41: 3263-3272.

22. Anand Prabu A, Alagar M. Thermal and Morphological Properties of Silicone-Polyurethane-Epoxy Intercrosslinked Matrix Materials. J Macromol Sci Part A: Pure Appl. Chem. 2005; 42: 175-188.

23. Murias P, Maciejewski H, Galina H. Epoxy resins modified with reactive low molecular weight siloxanes. Europ. Polym. J. 2012; 48: 769-773.

24. Gong W, Zeng K, Wang L, Zheng S. Poly(hydroxyl ether of bisphenol A)-block-polydimethylsiloxane alternating block copolymer and its nanostructured blends with epoxy resin. Polymer 2008; 49: 3318-3326.

25. Frohlich J, Thomann R, Mulhaupt R. Toughened Epoxy Hybrid Nanocomposites Containing Both an Organophilic Layered Silicate Filler and a Compatibilized Liquid Rubber. Macromolecules 2003; 36: 7205-7211.

26. Fröhlich J, Thomann R, Gryshchuk O, Karger-Kocsis J, Mülhaupt R. High-performance epoxy hybrid nanocomposites containing organophilic layered silicates and compatibilized liquid rubber. J. Mater. Sci. 2004; 92: 3088-3096.

27. Romo-Uribe A, Arcos-Casarrubias JA, Flores A, Valerio-Cardenas C, Gonzalez AE. Influence of rubber on the curing kinetics of DGEBA epoxy and the effect on the morphology and hardness of the composites. Polym. Bull. 2014; 71: 1241-1261.

28. Arcos-Casarrubias JA, Reyes-Mayer A, Guardian-Tapia R, Castillo-Ocampo P, Romo-Uribe A. Rubber Nanodomains Reinforced Epoxy Resin. MRS Advances 2016; 1: 1571-1576. DOI: 10.1557/adv.2016.297

29. Romo-Uribe A, Arcos-Casarrubias JA, Reyes-Mayer A, Guardian-Tapia R. PDMS nanodomains in DGEBA epoxy induce high flexibility and toughness. Polym. Plast. Techn. Eng. 2017; 56: 96-107, http://dx.doi.org/10.1080/03602559.2016.1211691

30. Flores A, Ania F, Balta-Calleja FJ. From the glassy state to ordered polymer structures. A microhardness study. Polymer 2009; 50: 729-746

31. ImageJ™ is image analysis software developed by the US National Institutes of Health. http://imagej.nih.gov/ij/

32. R. Castillo-Perez, A. Romo-Uribe, Diseño y construcción de un instrumento para medir ángulo de contacto, *Memorias del XVIII Congreso Internacional Anual de la SOMIM*, (2012) http://somim.org.mx/articulos2010/memorias/memorias2012/articulos/pdfs/A3/A3_269.pdf ISBN: 978-607-95309-6-9: 772-779

33. Puglia D, Kenny JM. Cure kinetics of epoxy/rubber polymer blends, in *Handbook of epoxy blends* (Parameswaranpillai J, Woo EM, Hameed N, Piontek J eds.) Springer, Switzerland, 2015

34. Romo-Uribe A. Dynamic mechanical thermal analysis of epoxy/thermoplastic blends, in *Handbook of epoxy blends* (Parameswaranpillai J, Woo EM, Hameed N, Piontek J eds.) Springer, Switzerland, **2016**. DOI: 10.1007/978-3-319-18158-5_23-1

35. Ratna D, Simon GP. Mechanical characterization and morphology of carboxyl randomized poly(2-ethyl hexyl acrylate) liquid rubber toughened epoxy resins. Polymer 2001; 42: 7739-7747

36. Agarwal M, Arif M, Bisht A, Singh VK, Biswas S. Investigation of toughening behavior of epoxy resin by reinforcement of depolymerized latex rubber. Sci. Eng. Compos. Mater. 2015; 22: 399-404

37. Gleghorn JP, Lee CSD, Cabodi M, Stroock AD, Bonassar LJ, Adhesive properties of laminated alginate gels for tissue engineering of layered structures. Journal of Biomedical Materials Research Part A, 2008; 85A: 611-618

38. Phillips MG. Simple geometrical models for Young's modulus of fibrous and particulate composites. Compos. Sci. Techn. 1992; 43: 95-100

39. Miwa M, Takeno A, Hara K, Watanabe A. Volume fraction and temperature dependence of mechanical properties of silicone rubber particulate/epoxy blends. Composites 1995; 26: 371-377

40. Barcia FL, Abraho MA, Soares BG. Modification of epoxy resin by isocyanate-terminated polybutadiene. J. Appl. Polym. Sci. 2002; 83: 838-849

41. Mathew VS, George SC, Parameswaranpillai J, Thomas S. Epoxidized natural rubber/epoxy blends: phase morphology and thermomechanical properties. J. Appl. Polym. Sci. (2014) 131: 399-406

42. Thomas R, Abraham J, Thomas PS, Thomas S. Influence of carboxyl-terminated (butadiene-co-acrylonitrile) loading on the mechanical and thermal properties of cured epoxy blends. J. Polym. Sci. 2004; 42: 2531–2544

Graphical Abstract

Functional PDMS enhanced strain at fracture and toughness of DGEBA epoxy resin

A Romo-Uribe, K Santiago-Santiago, A Reyes-Mayer

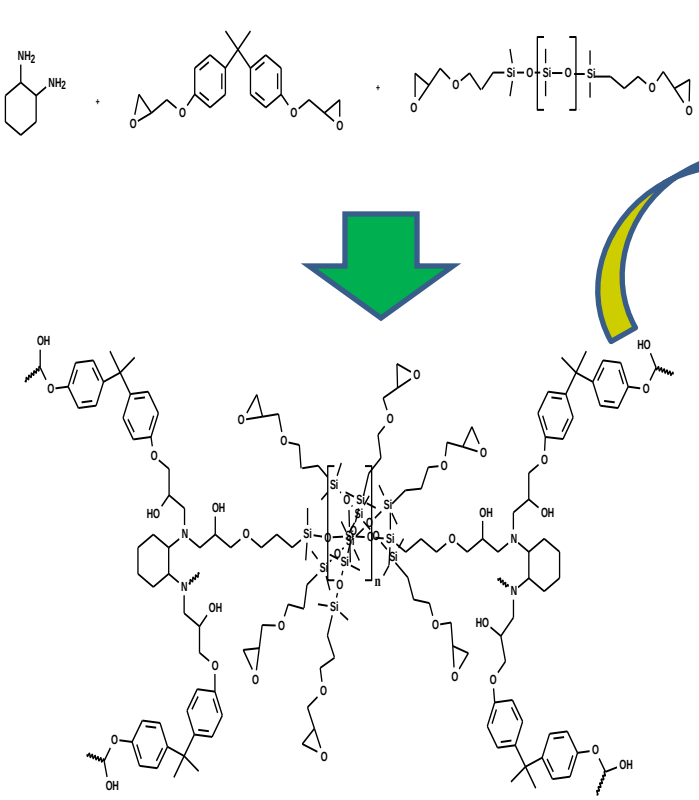

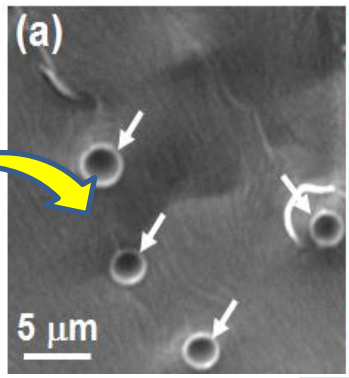

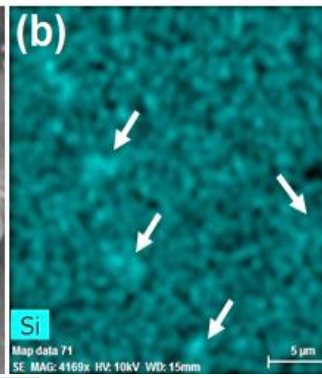

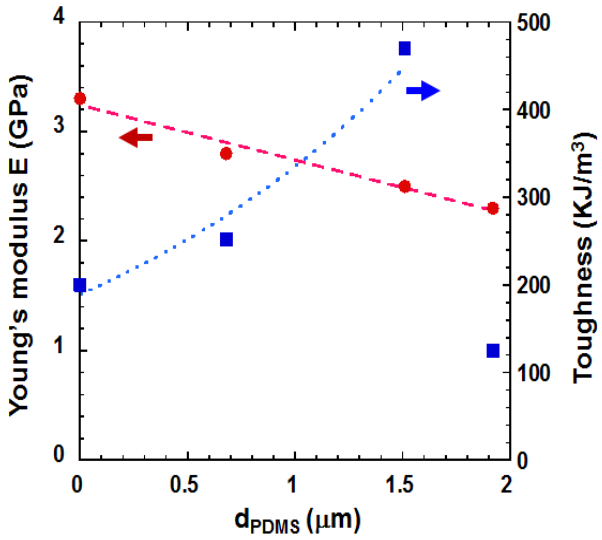

Highlights

Functional PDMS enhanced strain at fracture and toughness of DGEBA epoxy resin

A Romo-Uribe, K Santiago-Santiago, A Reyes-Mayer & M Aguilar-Franco

- Ether-terminated PDMS increased strain at fracture and toughness of epoxy by twofold
- PDMS droplet size range from 0.6 to 1.8 μm
- Flexural modulus scaled with PDMS droplet size